Arabian Journal of Chemistry (2016) 9, 274–286

King Saud University

Arabian Journal of Chemistry

www.ksu.edu.sa
www.sciencedirect.com

REVIEW

Influence of graphene oxide on mechanical, morphological, barrier, and electrical properties of polymer membranes

Ali Ammar [a], Abdullah M. Al-Enizi [b], Mariam AlAli AlMaadeed [c], Alamgir Karim [a,*]

[a] Polymer Engineering Academic Center, The University of Akron, 250 S. Forge St., Akron, OH 44325-0301, USA
[b] Department of Chemistry, Faculty of Science, King Saud University, PO Box 2455, Riyadh 11451, Saudi Arabia
[c] Center for Advanced Materials, Qatar University, PO Box 2713, Doha, Qatar

Received 9 April 2015; accepted 12 July 2015
Available online 22 July 2015

KEYWORDS

Graphene oxide;
Polymer;
Mechanical;
Morphology;
Barrier;
Properties

Abstract This paper expresses a short review of research on the effects of graphene oxide (GO) as a nanocomposite element on polymer morphology and resulting property modifications including mechanical, barrier, and electrical conductivity. The effects on mechanical enhancement related to stress measurements in particular are a focus of this review. To first order, varying levels of aggregation of GO in different polymer matrices as a result of their weak inter-particle attractive interactions mainly affect the nanocomposite mechanical properties. The near surface dispersion of GO in polymer/GO nanocomposites can be investigated by studying the surface morphology of these nanocomposites using scanning probe microscopy such as atomic force microscope (AFM) and scanning electron microscope (SEM). In the bulk, GO dispersion can be studied by wide-angle X-ray scattering (WAXD) by analyzing the diffraction peaks corresponding to the undispersed GO fraction in the polymer matrix. In terms of an application, we review how the hydrophilicity of graphene oxide and its hydrogen bonding potential can enhance water flux of these nanocomposite materials in membrane applications. Likewise, the electrical conductivity of polymer films and bulk polymers can be advantageously enhanced via the percolative dispersion of GO nanoparticles, but this typically requires some additional chemical treatment of the GO nanoparticles to transform it to reduced GO.

* Corresponding author. Tel.: +1 330 9728324; fax: +1 330 9723406.
E-mail address: alamgir@uakron.edu (A. Karim).
Peer review under responsibility of King Saud University.

Production and hosting by Elsevier

http://dx.doi.org/10.1016/j.arabjc.2015.07.006

Contents

1. Introduction

It is well known that blending in well-dispersed additives and fillers to polymers can substantially improve the mechanical and physical properties of the polymer composites (Liu et al., 2014). We examine a nanomaterial of much recent interest, graphene oxide (GO) in this context in forming polymer nanocomposites. Graphene oxide GO is produced by introducing graphite to oxidation agents that add oxygenated functionalities to the graphite structure and exfoliates the layers, thereby improving its dispersion in water. Recently, GO has emerged as one of the most attractive nanofiller in polymer nanocomposite technology due to the notable improvement and enhancement of mechanical, thermal, and electrical properties of many nanocomposites, improvements that could lead to innovative solutions for many applications (Zhu et al., 2010; Gómez-Navarro et al., 2007; Liu et al., 2009; Dikin et al., 2007; Lei et al., 2012; Sun et al., 2008; Marcano et al., 2010; Satti et al., 2010; Park et al., 2009; Venugopal et al., 2012; Wang et al., 2010; Hu et al., 2010; Zinadini et al., 2014; Jin et al., 2015; Gudarzi and Sharif, 2012; Dreyer et al., 2010; Compton et al., 2012). For instance, in water filtration applications, GO could potentially solve the serious obstacle of polymer membrane fouling by biological species. GO can play the role of anti-biofouling of nanocomposite membranes because it can alter the smoothness of the membrane surface, and also due to its hydrophilicity and electrostatic repulsion characteristics, all of which can disfavor bio-adsorption or even induce bio-degradation (Lee et al., 2013). While GO is highly attractive as a nanofiller material, there are other nanoparticles in this family of graphitic nanomaterials that lend themselves to enhancing properties of nanocomposites in general. In this regard as examples, graphene, graphene oxide and reduced graphene oxide nanosheets and nanotubes can have different interactions with many polymers at high loading due to the differences of their surface functional group. For example, reduction of graphene oxide to its "r-GO" form is one of the interesting nanoparticles due to its similar electrical properties to graphene. r-GO is produced by removing (reducing) functional group of GO using chemical or thermal treatments (Pei and Cheng, 2012). However, the dispersion of r-GO in polymeric and other materials is a notable challenge, hence it is typically reduced in situ, while GO is conveniently dispersed in water and other hydrogen bonding polar solvents. Note also that GO has largely insulating properties. GO improves the performance of hydrogen, H_2 and oxygen, O_2 permeability and also increases the proton conductivity of polyimides (PI) membranes due to the interaction between sulfonic functional group and GO (Jiang et al., 2012). GO has also been shown to have useful properties as nanosheets for bio-nanotechnology applications such as drug delivery, anti-bacteria, and DNA sensors (Wang et al., 2010; Ma et al., 2011).

As mentioned, polymeric membranes in various water treatment applications have different types of fouling problems, most commonly due to the natural organic materials. The hydrophilicity modification of these membranes by adding GO is considered to be a viable solution to this problem (Forati et al., 2014). One of the most commonly used polymers for water filtration is Polysulfone, PSf due of its resistance to high pH, and harsh chemicals. In addition to enhanced transport barrier, PSf has good mechanical and thermal properties, which preserves the membrane for a longer lifetime thereby reducing its lifetime cost in applications (Ganesh et al., 2013; Ionita et al., 2014; Zhao et al., 2013). However, PSf is a naturally hydrophobic material, so that dispersing graphene oxide in PSf to form GO/PSf nanocomposite membranes could be a key to changing the surface properties of Polysulfone and making it more hydrophilic (Yang et al., 2006). In contrast, the addition of carbon nanotubes, CNTs to Polysulfone can also improve the properties of these membranes for enhanced mechanical and thermal properties, but the high cost of CNTs compared to GO limits their uses (Voicu et al., 2013). Furthermore, CNTs have weak dispersion in solvents and polymers while GO has good dispersion in organic solvents and polymers compared to CNTs (Zhu et al., 2012; Wang et al., 2011).

Another interesting polymer that can be used as a commercial or laboratory ultrafiltration membranes is Polyethersulfone (PES). Like many polymers, it however has a fouling problem due to a lack of hydrophilicity, which adversely impacts its water permeability properties. However, the addition of GO into PES matrix improves the hydrophilicity of the membrane leading to better water permeability (Zinadini et al., 2014). Furthermore, polyvinylidene fluoride (PVDF) is also used as a nanofiltration membrane due to its thermal stability and easy to control surface structure (morphology). Similar to PES polymer, PVDF has the same fouling difficulty and likewise, with adding GO it can be improved (Xu et al., 2014).

In the chemical industry, aromatic/aliphatic separations are usually done by traditional separation like distillation, that however cost a lot of energy. Polymer membranes such as Poly(vinyl alcohol) PVA has the possibility to make these

separation processes more simple and low cost. Nonetheless, PVA has a poor interaction with aromatics due to the semicrystallinity of PVA. By adding GO one can reinforce the polymer membrane properties for better separation because of the introduction of oxygen functional group (Wang et al., 2014). Furthermore, Nafion or sulfonated aromatic poly(ether ether ketone)s SPEEKs are used in large scale for direct methanol fuel cells, DMFCs due to their many properties such as mechanical, thermal and chemical properties (Choi et al., 2012). This class of polymers still suffers from a major problem, which is the high permeability of methanol between the anode and cathode causes the fuel cells to have low efficiency. Addition of GO nanoparticles is found to provide a solution for this system as well, as the GO improves and changes the permeability of methanol (Yuan et al., 2014; Jiang et al., 2013; Chien et al., 2013).

The dispersion of graphene oxide in the polymer matrix is very important to the membrane properties. Furthermore, getting good dispersion also depends on the casting solvent used to dissolve the polymer. Paredes et al. (2008) investigated the stability of graphite oxide dispersion in different solvents. They prepared graphite oxide in water, N,N-dimethylformamide DMF,N-methyl-2-pyrrolidone NMP, tetrahydrofuran, ethylene glycol, and ethanol with concentration of 0.5 mg mL^{-1} using ultrasonication bath followed by aging the solutions for several weeks for characterization. As shown in Fig. 1, the UV–vis absorption spectroscopy results indicate that the graphite oxide has excellent dispersion and long-term stability in water, which gives the highest absorption intensity, followed by DMF and NMP. However, comparing to carbon nanotubes CNTs, GO has less temporal (time) stability in ethanol due to the dimensional size of GO, i.e. CNTs are considered as 1D and GO are 2D nanoparticles (Kim et al., 2012). Furthermore, the hydrogen bonding in GO is greater than CNTs, which makes it aggregate faster, thus to a larger extent with time in the solvent.

Various structural models of GO have been studied for decades. Fig. 2 illustrates the structural details of GO according to the different model of Lerf–Klinowski, Nakajima–Matsuo, Hofmann, Ruess, and Scholz–Boehm (Szabó et al., 2006). However, Lerf–Klinowski is the model that many scientists agree as the most appropriate model among all of these models. Basically, in this model graphene oxide is graphene (separated layers of graphite) with some functional groups deposited on the surface layers. These functional groups include carboxylic acid groups, (COOH) and hydroxyl groups, (OH) attached on the aromatic groups at locations where it is connected to each other by epoxide

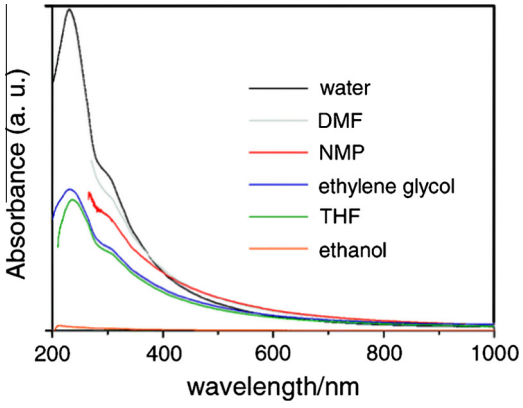

Figure 1 UV–vis absorption spectra of graphite oxide dispersed in different solvents after ultrasonication for 1 h. These dispersed solutions were kept for 3 weeks before the measurements [reproduced with permission from Paredes et al. (2008)].

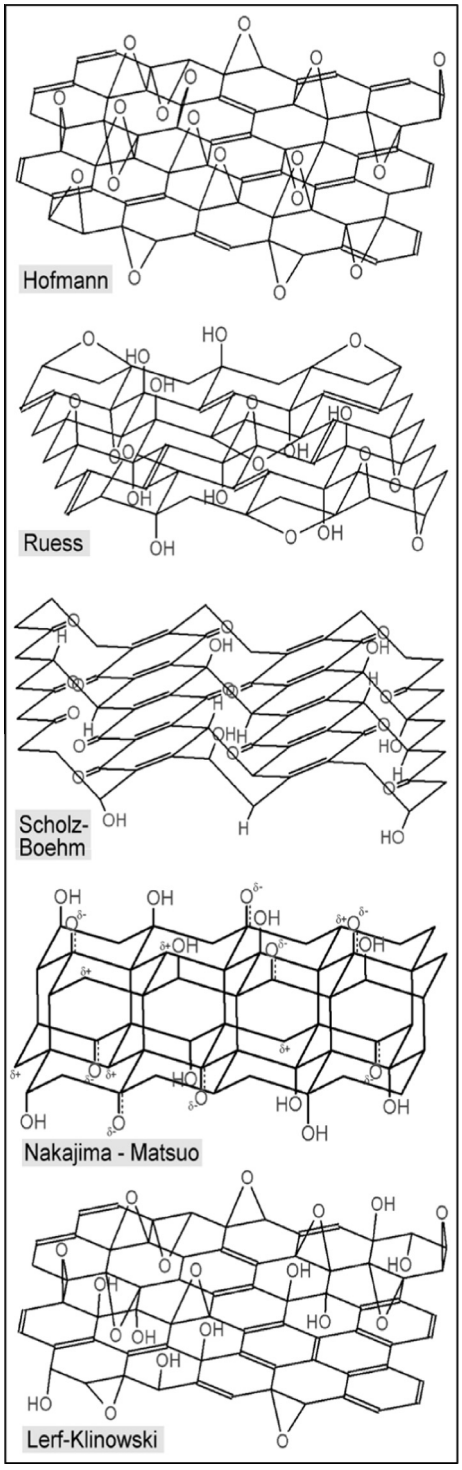

Figure 2 Different structure models of GO [reproduced with permission from Szabó et al. (2006)].

groups and double bonds (Lerf et al., 1998; Dreyer et al., 2014; He et al., 1998).

1.1. Synthesis of graphene oxide (GO)

Preparing graphene oxide in the laboratory can be done by the modified Hummers method (Xu et al., 2008). There are three main steps of graphene oxide synthesis by Hummers method as shown in Fig. 3 (Garg et al., 2014). The first step is oxidation of graphite powder to attach functional groups. In this step, graphite powder is added to a mixture of Potassium persulfate $K_2S_2O_8$, phosphorus pentoxide P_2O_5, and sulfuric acid H_2SO_4.

The solution is kept at 80 °C for approximately 4.5 h on a hot plate, and then the mixture is cooled to room temperature and diluted by adding deionized DI water and kept overnight in the hood. The mixture is cleaned off residual acid by a filtration process of the solution using a 0.2 μm nylon filter using DI water, monitored each time using a pH meter. After these steps the solution is kept overnight for drying at room temperature to obtain the pre-oxidized graphite product. After drying, the product is treated by the Hummer's method for controlled oxidation. The graphite powder is added to 120 ml sulfuric acid, H_2SO_4 gradually under an ice bath to reach 0 °C with continuous stirring. After reaching 0 °C, 15 g of potassium permanganate is added very slowly with stirring, and the temperature was kept below 20 °C. The mixture is then heated at 35 °C for a fixed amount of time while stirring constantly, and then diluted by adding 250 ml of DI water very slowly under the ice bath. The reason for adding DI water to sulfuric acid slowly is to avoid a significant rise in temperature. After addition of DI water, the solution is stirred for 2 h with the addition of an extra 0.7 L of DI water. 20 ml of hydrogen peroxide is added slowly with continuous stirring for several minutes and then filtered. The mixture is then washed with about 1 L of 1:10 HCl:H_2O (aqueous solution) to remove all metallic ions and then washed by 1 L of DI water to remove the acids. The last step is purification of the product via dialysis for 2 weeks to remove the remaining metal species and acids to get a dispersion of graphene oxide (GO).

2. Mechanical properties

As is well known, nanoadditives such as carbon black or silica nanoparticles can be added to rubber to improve their mechanical properties needed in tires industry. In this regard, graphene oxide is one of these additives that can enhance mechanical properties of polymer/elastomer composites. For example, octadecylamine modified graphene-oxide (OMGO) polybutadiene has been studied by Zhang et al. (2014). They used dynamic mechanical analysis or DMA to study the modulus of the OMGO-polybutadiene composites. As shown in Fig. 4, OMGO loading decreased the shear stress modulus due to the aggregation of these nanofillers aided by their weak interaction with polybutadiene. Despite significant

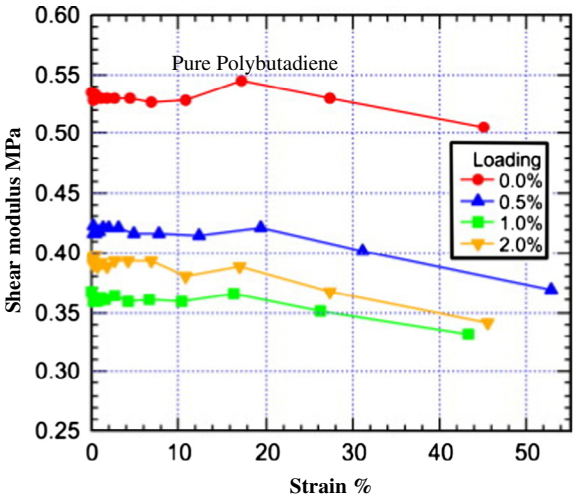

Figure 4 Dynamic mechanical analysis DMA data show reduction in modulus of polybutadiene with adding OMGO filler [adapted from Zhang et al. (2014)].

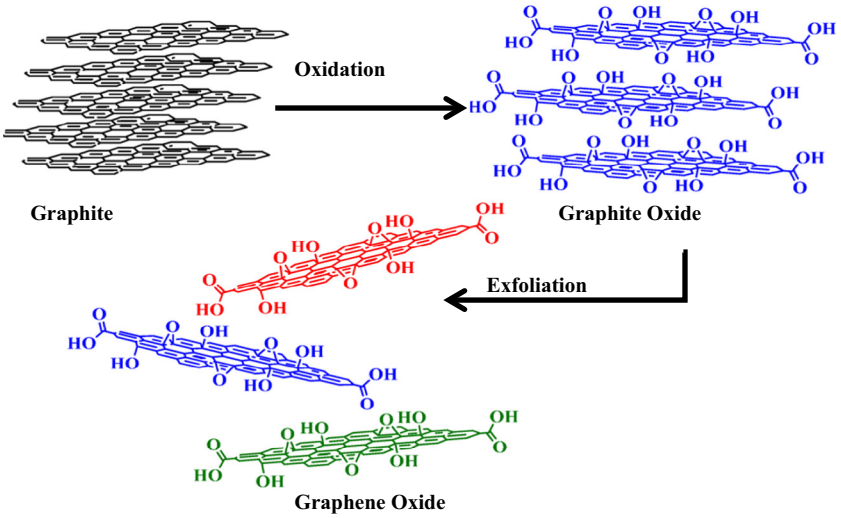

Figure 3 The three steps of preparing graphene oxide GO from graphite [adapted from Garg et al. (2014)].

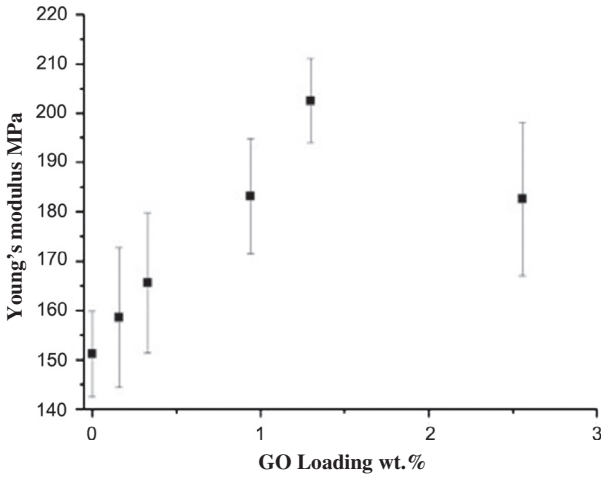

Figure 5 Young's modulus of PSf membrane for various GO contents (error bar: standard deviation, $n = 5$) [adapted from Lee et al. (2013)].

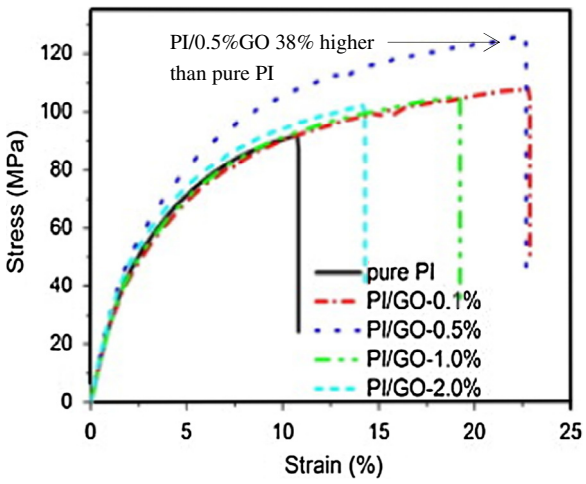

Figure 6 Tensile strength of PI, and PI/GO with different loading versus strain [adapted from Chen et al. (2015)].

aggregation, the addition of OMGO decreased the oxidation of the polymer. On the other hand, another group (Lee et al., 2013) prepared PSf/GO nanocomposite membranes and found that adding GO to the polymer matrix increased the mechanical strength as shown in Fig. 5. Unfortunately, increasing the amount of GO to 2.6 wt.% led to weaker mechanical strength due to aggregation of GO in the PSf matrix.

Furthermore, Ionita et al. (2014) studied the mechanical properties of PSf/GO membranes by dispersing the nanocomposite materials into N,N-dimethylformamide (DMF) solvent and casting the solution on a glass plate. After casting they immediately immersed it in a water bath. This method, known as phase inversion, leads to membranes having an asymmetric structure derived from a solvent/non-solvent fast exchange process. They found an increase in tensile modulus and tensile strength at low concentration of GO as shown in Table 1. However, at 2 wt.% GO, the mechanical properties decreased due to the aggregation of GO. These studies lead to the conclusion that generally GO has poor dispersion at high loading in most polymer matrices.

Besides tires, the automotive industries currently use membranes such as DuPont's Nafion membranes in batteries based on direct methanol fuel cells. Yet, these membranes have some disadvantages such as high cost, corrosion, and loss of conductivity at temperature above 100 °C. Replacement of Nafion by polyimides (PIs) is suggested as a solution to these problems; however, the PIs need to be augmented by nanofillers to improve their properties in many applications, such as for the spacecraft industry (Tseng et al., 2011; Park et al., 2014).

Table 1 Tensile modulus, tensile strength of PSF and PSF-GO composite materials (Ionita et al., 2014).

Sample	GO content (wt.%)	Tensile modulus (MPa)	Tensile strength (MPa)
PSf	0	187 ± 11	3.33 ± 0.28
PSf/GO	0.25	201 ± 26	4.06 ± 0.53
PSf/GO	0.5	199 ± 14	3.67 ± 0.33
PSf/GO	1	218 ± 30	3.84 ± 0.39
PSf/GO	2	144 ± 9	2.36 ± 0.41

Most commonly, PIs are widely used in gas separation applications due to their high thermal stability and enhanced mechanical properties (Kapantaidakis et al., 1999). However, polyimide has the problem of plasticization by CO_2 in gas filtration applications, and adding GO to the polymer matrix can improve/solve these material problems (Kapantaidakis and Koops, 2002). Chen et al. (2015) have studied the addition of graphene oxide to polyimide and measured the mechanical properties of these nanocomposites. As indicated in Fig. 6, the tensile strength of PI increased with added GO content due to the good dispersion and interaction of GO with PI in these nanocomposites. As with many nanocomposite systems, adding 1% and 2% by weight of GO showed slightly decreased mechanical properties due to aggregation of GO at a "high content" (note that the definition of high content for nanofillers is clearly different than traditional fillers). Not only can addition of GO improve the mechanical properties, but also the (chemical) treatment of GO can improve and alter the mechanical properties of polymer membranes. Xu et al. (2014) functionalized GO with silane and studied their mechanical properties compared to unfunctionalized GO. PVDF/GO as well as silane functionalized-GO membranes were prepared by phase inverse of cast films. As shown in Fig. 7, it is obvious that f-GO membranes had much better mechanical properties than GO membranes. The reason behind this is that the silane surrounding the GO particles prohibits them from aggregating.

Another important class is Nafion membranes that are used in large scale in fuel cells due to their intrinsic high conductivity in wet state at elevated temperatures. Lee et al. (2014) prepared Nafion/GO membranes by adding GO to form nanocomposite membranes and studied the effect of GO on Nafion membranes. As shown in Fig. 8, the mechanical properties improved drastically, but they did not explain the reason behind it. It may be due to the hydroxyl interaction between

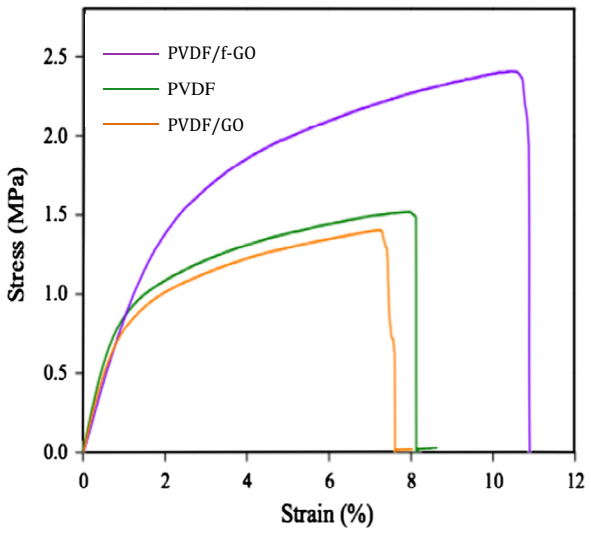

Figure 7 Stress–strain curves of nascent membranes and 1 wt.% additive-mixed PVDF membranes [adapted from Xu et al. (2014)].

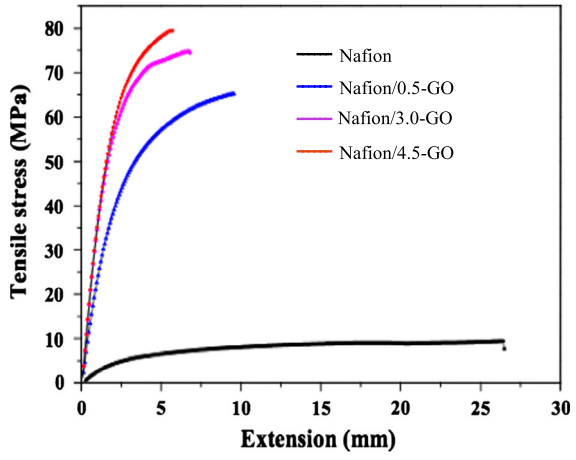

Figure 8 Tensile strength of Nafion/GO nanocomposite membranes with different contents of GO loading [adapted from Lee et al. (2014)].

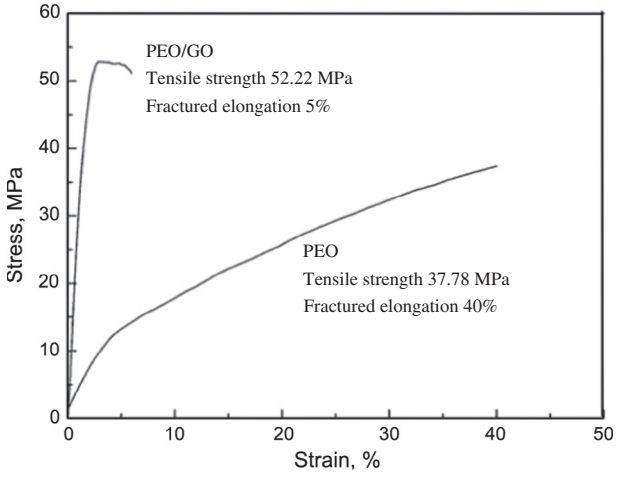

Figure 9 Stress–strain curves of the PEO/GO nanocomposite and PEO membranes [adapted from Cao et al. (2011)].

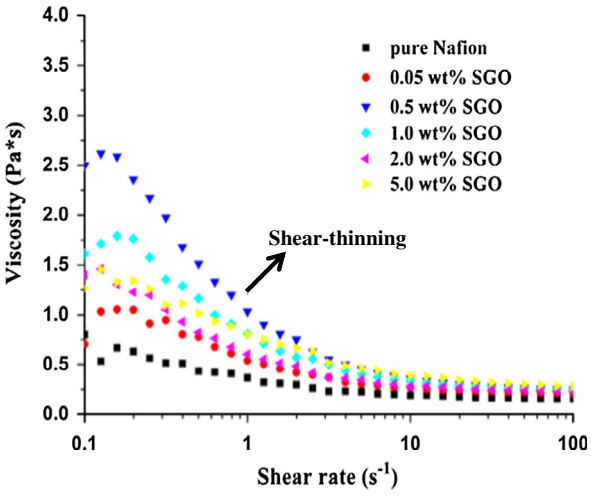

Figure 10 Rheological spectra of pure Nafion solution and different SGO loadings of SGO/Nafion solutions [adapted from Chien et al. (2013)].

the Nafion and GO particles, since both entities have OH functional group.

Furthermore, Cao et al. (2011) prepared poly (ethylene oxide)/graphene oxide PEO/GO nanocomposite membranes to study the effect of GO on mechanical properties as well. By using tensile testing, they found that PEO/GO had increase in tensile strength and Young's modulus compared to pure PEO membranes as shown in Fig. 9. The attractive interaction between the polymer and functional group on GO is a key reason behind the enhancement. However, increased GO loading makes the polymer stronger but more brittle.

Graphene oxide also has an effect on the solution viscosity of the polymers. Chien et al. (2013) studied the effect of sulfonated graphene oxide, SGO on Nafion rheology. As shown in Fig. 10, the solution viscosity of the polymer increased with increasing SGO loading comparing to neat Nafion. The improvement occurred because of the cooperative bonds interaction of Nafion and SGO functional group. The aggregation of high content SGO is provided as the reason for the viscosities shifting down for 1, 2 and 5 wt.% loading of SGO.

Chitosan (CS) is an interesting polymer for many applications such as membrane separations, packaging materials, and drug delivery. In addition, cross-linking CS can improve the properties of CS due to the interaction between amine groups on CS and other group that makes it stronger. Yet, GO has a drastic enhancement effect on CS membranes due to the strong interaction between epoxy and amino groups. A set of researchers have done the studies on the effect of GO on CS membranes and tested their mechanical properties. As shown in Fig. 11, the tensile strength of crossed-linked CS membranes increased strongly with increasing GO content. The claimed reason behind this improvement is attributed to the bond formation after cross-linking reaction between GO and CS (Shao et al., 2013). Moreover, Justin and Chen have also studied the mechanical properties of CS/GO nanocomposites with different loading – 0, 0.25, 0.5, 1, 2, and 5 wt.% of GO. They found that GO developed better tensile strength in CS nanocomposites. Basically, the stress transfer from the CS chain to GO particles increased, due to the fact that GO

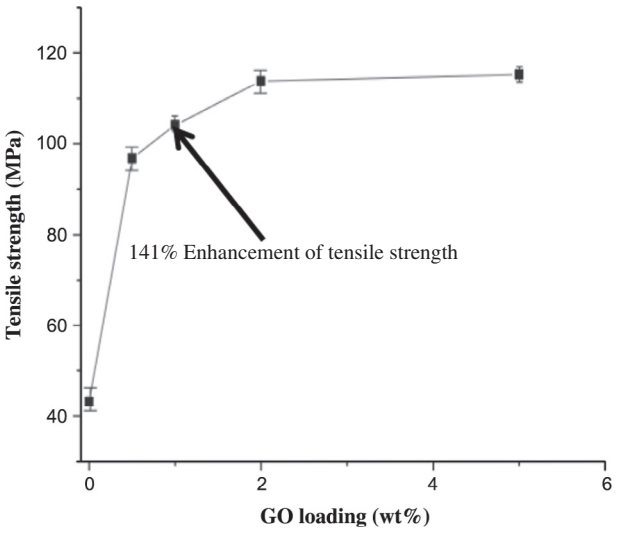

Figure 11 The effects of GO contain on the tensile strength of CS membranes [adapted from Shao et al. (2013)].

has a higher Young's modulus than CS. However, increasing GO content to 5 wt.% decreased the mechanical property because of the aggregation of the particles, i.e. poor dispersion (Justin and Chen, 2014).

3. Morphology and structural properties

Lee and coworkers also studied the effect of GO on the morphology of PSf membranes (Lee et al., 2013). Their membranes were prepared by sonication of different loading of GO in N-methyl pyrrolidone NMP and mixed with PSf. The polymer solutions were cast on a polyester non-woven fabric using a micrometric film applicator and then immersed in a water bath. As shown in Fig. 12, the pore size of PSf membrane increased with adding GO. Yet, the pore size of the membrane reduced at 2.6 wt.% of GO due to the fast solidification of the polymer during phase inversion between solvent and non-solvent. Additionally, it could be because of the viscosity increase due to adding large amounts of GO. Furthermore, Ganesh et al. (2013) investigated the surface morphology by using Atomic Force Microscopy AFM of PSf/GO nanocomposite membranes. They found that the surface has more roughness with GO loading as shown in Fig. 13. The reason behind that could be due to the fast exchange between solvent and non-solvent during the phase inverse process that impacts the porosity in the membrane.

Zhu et al. (2012) prepared polyimide, PI samples by adding reduced graphene oxide r-GO and studied the fractured surface morphology by scanning electron microscope SEM. As shown in Fig. 14, it is obvious that even for polyimide PI, adding r-GO increased the surface roughness compared to PI without r-GO films. They investigated the mechanical proper-

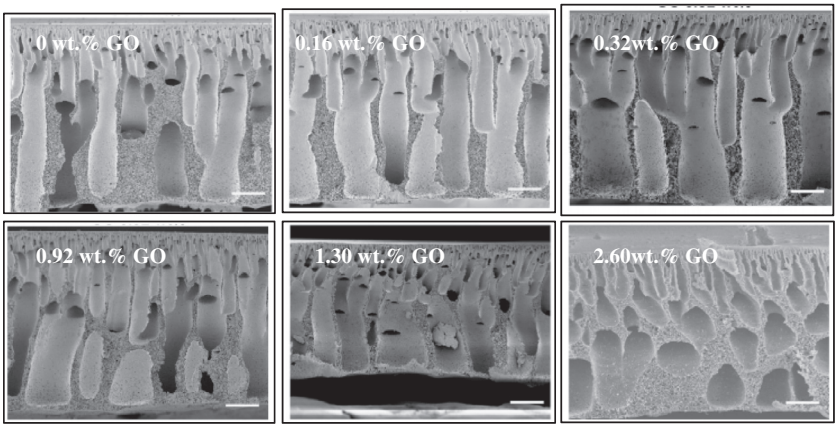

Figure 12 SEM images indicate the effect of GO on the membrane pore and membrane cross-sectional structure. Scale bars, 20 μm [adapted from Lee et al. (2013)].

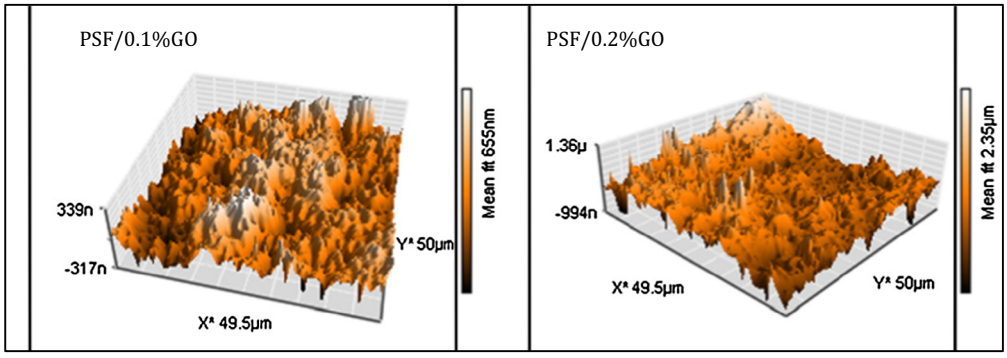

Figure 13 AFM images of PSf/GO mixed matrix membranes [adapted from Ganesh et al. (2013)].

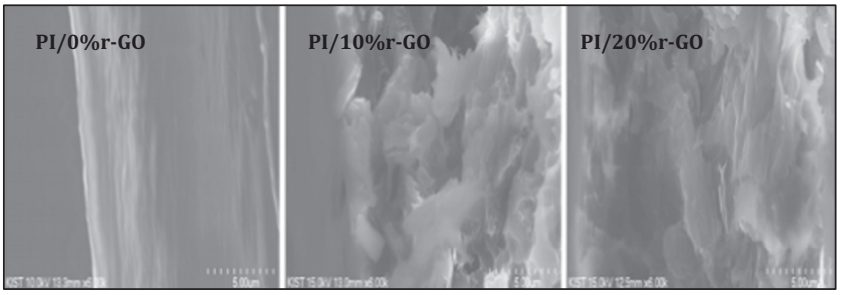

Figure 14 Scanning electron microscope micrographs of the fractured surfaces of PI/r-GO/PI composite PI: polyimide, r-GO: reduced graphene oxide [adapted from Zhu et al. (2012)].

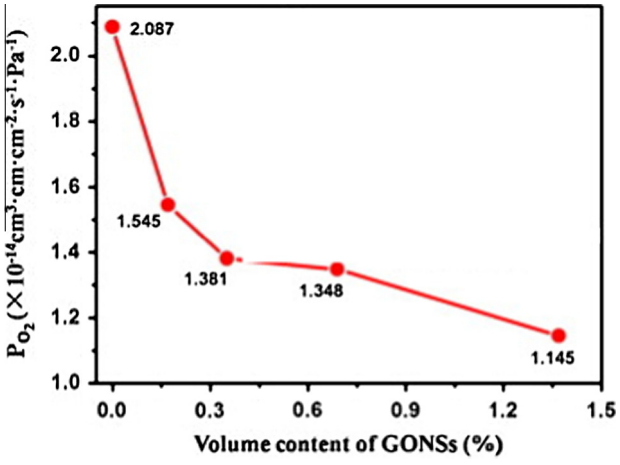

Figure 15 Decreasing of permeability of oxygen (PO_2) for neat PLA with GONS wt.% loading [adapted from Huang et al. (2014)].

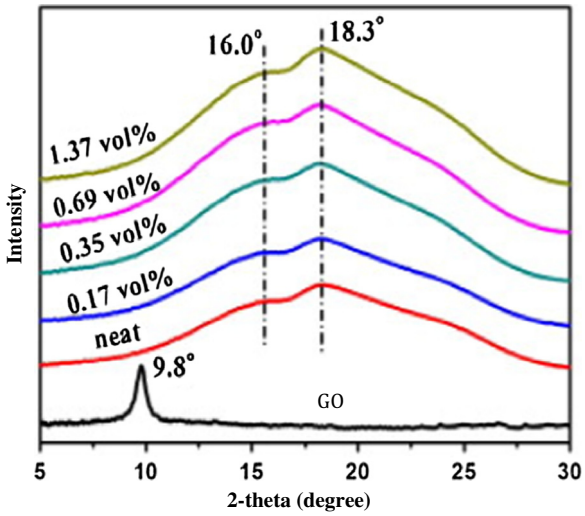

Figure 16 Wide-angle X-ray scattering WAXD of graphite oxide, neat PLA and its nanocomposites with different GONS wt.% loadings [adapted from Huang et al. (2014)].

ties aspects based on the notion that there is non-covalent interaction between PI and r-GO phases.

4. Barrier properties

Polymers that are used in the food industry have many challenges such as oxygen permeability. One such polymer is Poly(lactic acid) PLA. Huang et al. (2014) studied the effect of addition of graphene oxide nanosheets GONSs on oxygen barrier property of a PLA matrix. As shown in Fig. 15, the nanosheets of GONSs reduced the oxygen permeability dramatically due to the high degree of exfoliation of GONSs in the PLA matrix, which is conformed by wide angle X-ray scattering WAXS as shown in Fig. 16.

On the other hand, GO nanofillers enhance the permeability properties of water flux of cellulose acetate, CA membranes in water filtration applications. The main idea here is that the interaction between graphene oxide and cellulose acetate will mainly depend on hydrogen bonds as shown in Fig. 17. The presence of graphene oxide may disturb the pore size and pore distribution within the membrane framework. This interaction will lead to an increase in the water flux, which will prevent fouling problems of the surface membrane during the filtration process. Also, the addition of graphene oxide is expected to increase the nanomechanical properties of the membrane as well (Jeon et al., 2012). Kabiri and Namazi had done a study on nanocrystalline cellulose acetate/graphene oxide NCCA/GO composite films (Kabiri and Namazi, 2014). They examined the effect of addition of GO on mechanical properties of NCCA matrix. Addition of GO can improve the tensile strength, but yet, after adding more than a threshold amount of GO, the mechanical properties were reduced due to the orientation of GO sheets and the dispersion level of GO in NCCA, as shown in their SEM images. On the other hand, they studied the water vapor flux and found a decrease in water vapor flow through the films with increasing GO loading, due to the long pathway of water molecules through GO sheets. However, all studies anticipate that the controlled dispersion of the graphene oxide in the membrane is key to the proposed research. It has also been reported that there is a strong interaction between GO and CA in solution state that may be useful for membrane casting (Zhang et al., 2012).

Ganesh et al. (2013) also studied the hydrophilicity of GO/PSf nanocomposites using contact angle measurement. The water contact angle of neat Polysulfone is 70°. With GO loading into PSf matrix, the contact angle decreased to 65°, and 53° with increase of GO content to 1000 ppm, and 2000 ppm respectively. This is apparently due to the fact that

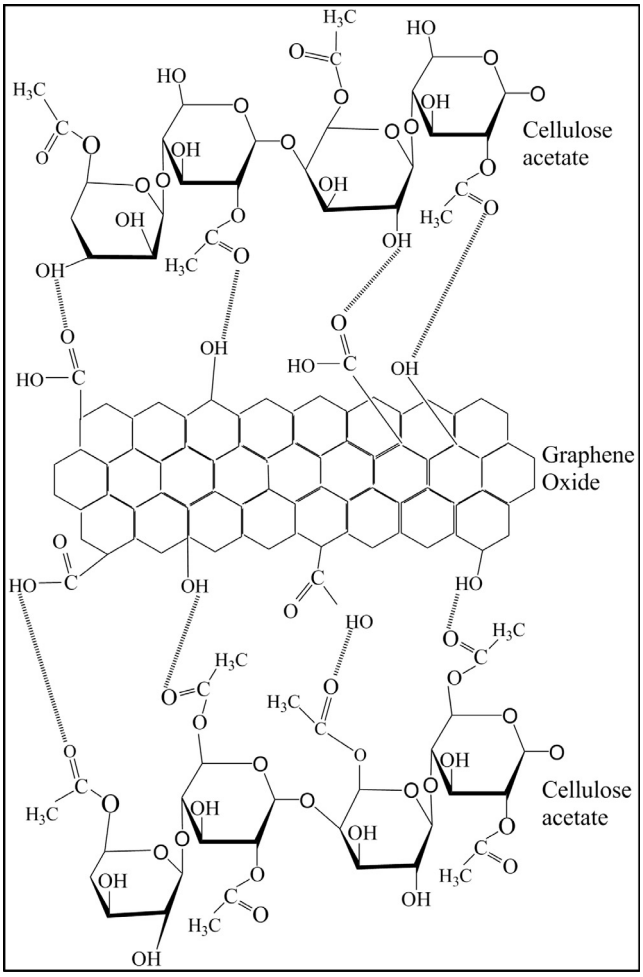

Figure 17 The interaction between cellulose acetate CA and graphene oxide GO [adapted from Kabiri and Namazi (2014)].

GO migrates to the surface during phase inverse preparation of membrane and so the surface became more hydrophilic due to the presence of OH group. Furthermore, they measured the effect of pH on water uptake with different loading of GO. As shown in Fig. 18, the water uptake increased with increasing pH due to the varying segregation of GO on the surface at different functional group concentrations apparently. The reaction at the surface can be summarized as the following (Ganesh et al., 2013).

I. The dissociation of carboxylic group attached to graphitic backbone

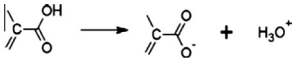

(1)

II. Dissociation of phenolic groups

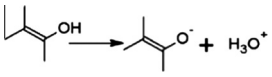

(2)

Eqs. (1) and (2) are responsible for the surface reaction between the GO and water, where the functional groups of GO produce a negative charge which increase the water uptake. On the other hand, Zhao et al. (2013) studied the effect of isocyanate-treated graphene oxide (iGO) on PSf membranes. The water flux of these membranes at a pressure of 100 kPa was found to be decreasing in water flux with increasing iGO loading as shown in Fig. 19. The reason for this decrease is due to the decrease in the surface pore size and modified pore structure by adding iGO content.

Moreover, Zinadini et al. (2014) reported the effect of GO on Polyethersulfone PES membranes. They prepared PES/GO nanocomposite membranes by phase inversion method of cast film solutions with different loading of GO. As shown in Fig. 20, the water contact angle measurements show a decrease of contact angle with increasing GO content, and this is due to the effect of GO on the surface making it more hydrophilic. However, at 1.0 wt.% loading of GO, the nanofilled film surface shows increasing contact angle due to the aggregation of

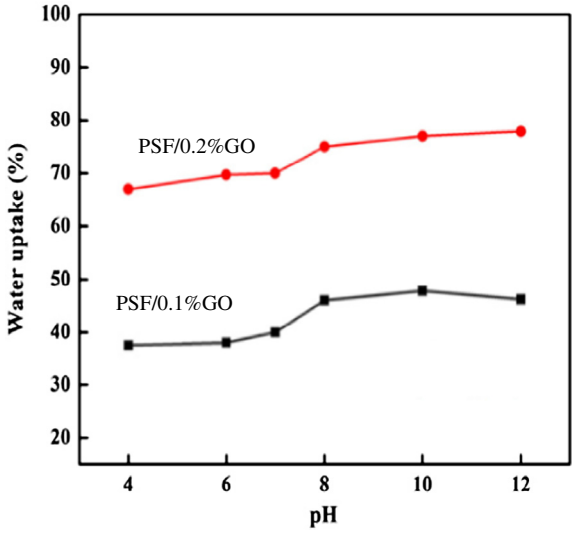

Figure 18 The effect of pH on water uptake for PSf/GO membranes [adapted from Ganesh et al. (2013)].

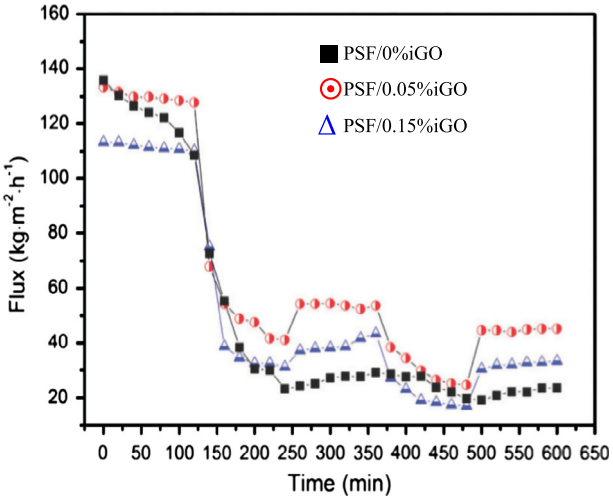

Figure 19 Water flux versus time for iGO blended PSF membranes at 100 kPa [adapted from Zhao et al. (2013)].

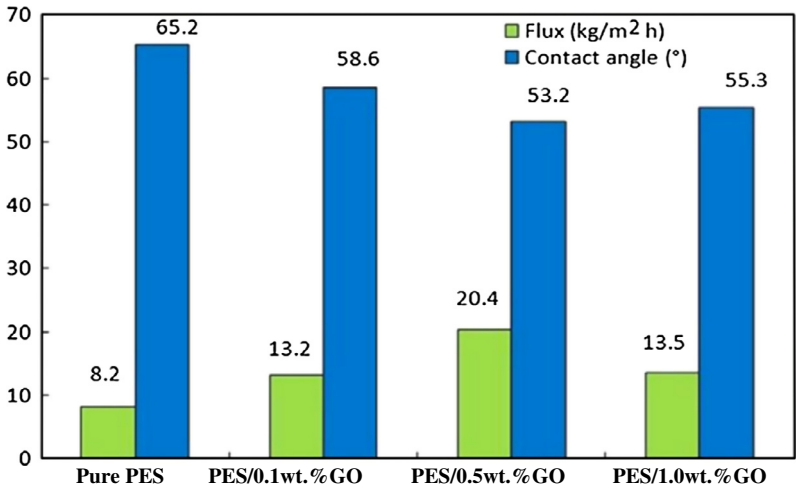

Figure 20 Pure water flux (after 60 min) and static contact angle of the prepared membranes. Where $M1 = 0.1$, $M2 = 0.5$, and $M3 = 1.0$ wt.% of GO [adapted from Zinadini et al. (2014)].

nanoparticles. Furthermore, they studied the water flux of these membranes and found that the water flux increased with increasing GO content, because of the formation of porosity with adding GO during the phase inverse method. At 1.0 wt.% of GO, there is a decrease in water flux due to the blocking of pores by adding high loading of GO, which they studied by the equation mentioned below:

$$\varepsilon = \frac{\omega 1 - \omega 2}{A \times l \times d_w} \tag{3}$$

where $\omega 1$ is the weight of the wet membrane; $\omega 2$ is the weight of the dry membrane; A is the membrane effective area (m^2); d_w is the water density (998 kg/m^3) and l is the membrane thickness (m).

Tseng et al. (2011) studied the permeability of methanol in sulfonated-polyimide/GO SPI/GO nanocomposite membranes. The experiment was performed under two different temperatures (30 °C and 80 °C) to study the effect of temperature on methanol permeability. They found that there is a decrease in methanol permeability with increasing GO loading at 30 °C as well as at 80 °C. The reason behind this decrease is that GO intercalates with the SPI matrix and is dispersed in it, which made methanol less permeable. On the other hand, it is different from water uptake that increased with increasing GO due to the negative charge and resulting hydrogen bonding between water and GO. Furthermore, Yuan et al. (2014) studied the methanol permeability in modified Nafion membranes used for direct methanol fuel cells DMFCs by layer by layer assembly of poly-(diallyldimethyl-ammonium chloride) (PDDA) and graphene oxide (GO) nanosheets on the surface of Nafion membranes. As shown in Fig. 21, the permeability of methanol decreased by 63% after using 2 bilayers modification compared to the neat Nafion because PDDA/GO functions as a blocking layer against methanol.

Water treatment by membrane bioreactors (MBRs) is attracting much attention compared to traditional processes due to their high separation and sludge resistance properties. However, polyvinylidene fluoride (PVDF) blended with GO can be one of the better membranes to use in MBRs due to its simultaneous high resistance to chemicals, hydrophilicity

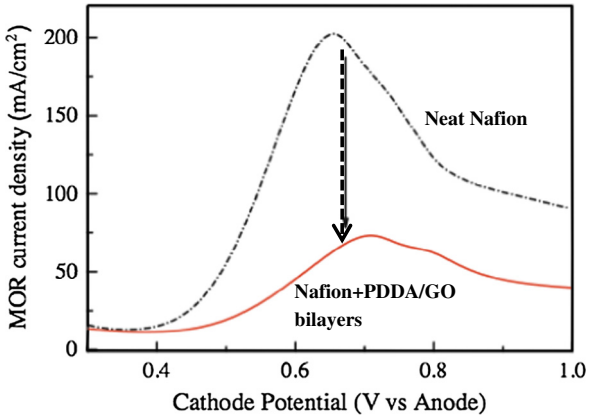

Figure 21 The limiting current density of methanol oxidation due to methanol crossover on the cathode of the MEA with pristine Nafion® membrane (a) and 2 bilayers modified composite membrane (b) [adapted from Yuan et al. (2014)].

Table 2 Parameters of commercial PVDF and composite membranes (Zhao et al., 2014).

Parameters	PVDF	PVDF/GO
Water permeability (Lm−2•h−1•bar−1)	171.12 ± 5.33	552.92 ± 6.54
Mean pore size (μm)	0.041 ± 0.007	0.089 ± 0.042
Maximum pore size (μm)	0.10 ± 0.032	0.66 ± 0.071
Contact angle (°)	78.30 ± 2.40	60.50 ± 1.80

and anti-fouling properties. Zhao et al. (2014) have studied the effect of GO on modified PVDF surface morphology, which is important for the separation process. As shown in Table 2, by adding GO to PVDF/GO membranes, the surface becomes more porous by adding GO to the polymer matrix, thereby increasing the water permeability. This increase in water permeability after adding GO to the polymer is due to the structural changes. The same group (Zhao et al., 2013) has done a study in another paper by using cross-sectional micrographs of SEM to illustrate this aspect. As shown in

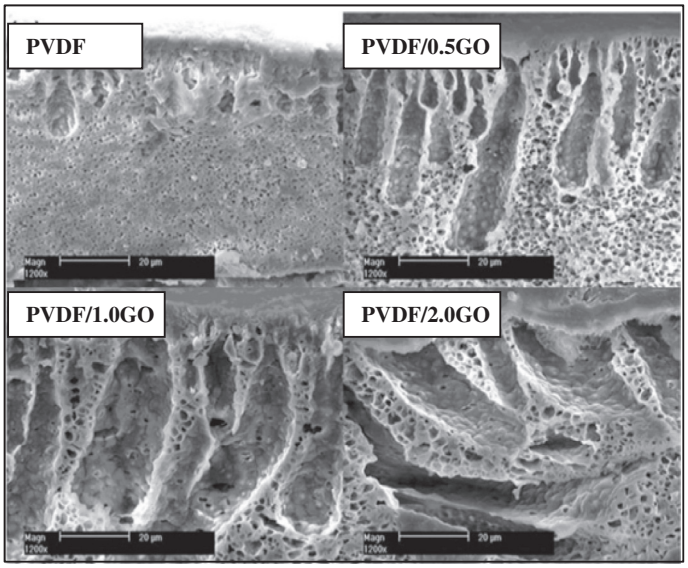

Figure 22 SEM images of cross-sectional morphologies for PVDF/GO UF membranes [adapted from Zhao et al. (2013)].

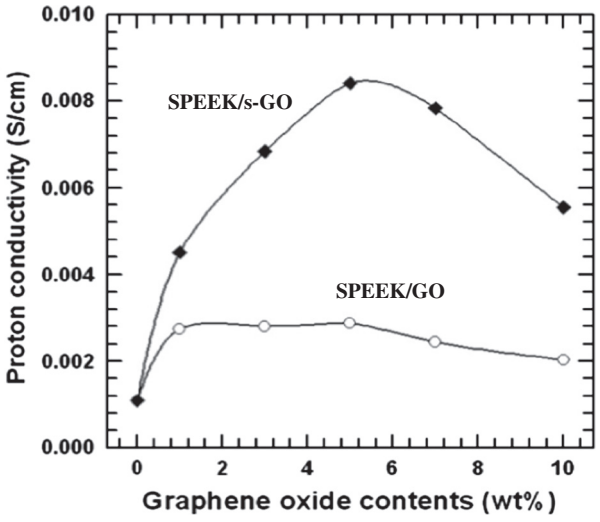

Figure 23 Proton conductivity of GO/SPEEK and s-GO/SPEEK membranes at 80 °C [adapted from Heo et al. (2013)].

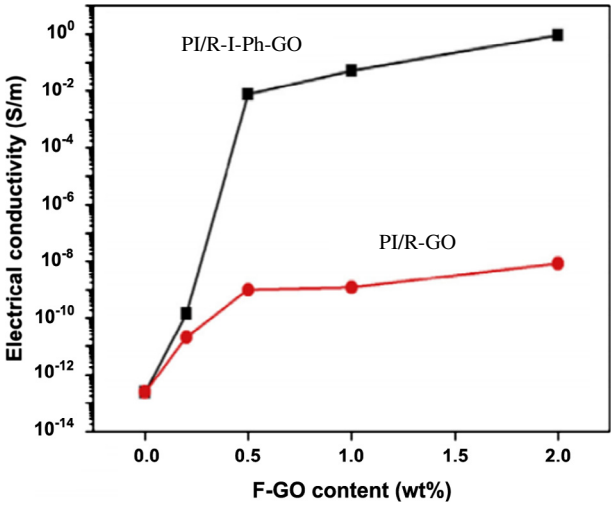

Figure 24 Electrical conductivity of functionalized GO filled PI nanocomposites with various contents of I-Ph-GO and GO [adapted from Park et al. (2014)].

Fig. 22, the structure became more finger-like with increased porosity of the membrane, where the micro-paths provide low resistance to water permeability.

5. Electrical conductivity properties

Graphene oxide is considered as a non-conductive material, and to improve its conductivity most of the oxygen groups should be removed to convert it to reduced graphene oxide. The reduction of GO is needed to reduce the interlayer spacing and removal of oxygen that contain the functional groups. Nevertheless, adding GO has a drastic enhancement effect on proton conductivity. Heo et al. (2013) investigated the effect of sulfonated graphene oxide S-GO on sulfonated Poly (ether ether ketone) PEEK, comparing to adding the GO without treatment, for applications where these membranes can be used in DMFCs. As indicated in Fig. 23, they found that the addition of S-GO increased the proton conductivity of the polymer membrane much more than by adding GO. A reasonability explained for this improvement is that the sulfonic functional group acts as percolative channels for the protons. However, the addition of S-GO can only be performed up to a critical amount, and after that it has detrimental blocking effects.

On the other hand, Park et al. (2014) investigated the effect of GO on electric conductivity of PI nanocomposite. Two methods were used to reduce GO. The first is iodo phenyl and phenyl functionalization of GO. In this approach, R-I-Ph-GO is prepared to create the surface functional group, followed by in situ polymerization. In the other method, there is thermochemical reduction to obtain R-GO. As shown in Fig. 24, the electric conductivity increased with increased

loading of GO. It is obvious from the graph that R-I-Ph-GO/PI films have higher electric conductivity compared to R-GO/PI films, due to sp^2-hybrid carbon network formation of graphene oxide. Thermochemical reduction of GO can affect its electric conductivity, yet, deoxygenation is enhanced by using R-I-Ph-GO, which improves the reduction of GO, acting as a catalyst to increase the conductivity of PI nanocomposites.

6. Conclusion and perspectives

In this review article, we have covered a brief summary of studies of graphene oxide GO as a nanocomposite element, and its effect on mechanical, morphology, barrier, and electric properties. GO has a strong influence on mechanical properties of polymer membranes due to their good dispersion and generally good interactions with many polymer matrices. However, higher dispersion of GO is difficult to reach after a certain amount of loading above which it adversely affects modulus, strength and surface wettability. Various studies are used to illustrate the morphology of polymer/GO nanocomposite films as shown in this review, with interpretations related to the properties reviewed. The review illustrates that the GO nanoparticles affect pore structure, surface roughness and surface wettability of the polymer membranes, which in turn is correlated with the membrane permeability properties, represented in their gas or liquid separation processes. Electric conductivity of GO filled polymers also showed improvement upon addition of reduced GO to different polymer matrices due to the intrinsic conductivity of these nanoparticles.

Looking toward the future, graphene oxide will become even more attractive for many applications in our daily life, e.g. gas and water molecular transport through laminar graphene oxide membranes (Xu et al., 2015). To a large extent, this will depend on good dispersion of GO at a large production scale, not only in laboratory scale. The cost of producing GO is also what limits its usage additionally, so finding ways to produce large amount at low cost needs to be investigated. While dispersion is a key issue, the stability of dispersion enabling GO functional groups is very important for its application with polymer composite such as water filtration membranes, such as chlorine stability for water filtration. Increased dispersion at high loading of GO is the main barrier to be overcome for many new applications of this promising class of nanomaterial.

Acknowledgments

The authors acknowledge the support of the ACS-#52997-ND7 Petroleum Research Foundation. The authors extend their sincere appreciations to the Deanship of Scientific Research at King Saud University for its funding this Prolific Research group (PRG-1436-14) for this graphene oxide based membranes review study.

References

Cao, Y.-C., Xu, C., Wu, X., Wang, X., Xing, L., Scott, K., 2011. J. Power Sources 196, 8377.
Chen, M., Yin, J., Jin, R., Yao, L., Su, B., Lei, Q., 2015. Thin Solid Films.
Chien, H.-C., Tsai, L.-D., Huang, C.-P., Kang, C., Lin, J.-N., Chang, F.-C., 2013. Int. J. Hydrogen Energy 38, 13792.
Choi, B.G., Huh, Y.S., Park, Y.C., Jung, D.H., Hong, W.H., Park, H., 2012. Carbon N.Y. 50, 5395.
Compton, O.C., Cranford, S.W., Putz, K.W., An, Z., Brinson, L.C., Buehler, M.J., Nguyen, S.T., 2012. ACS Nano 6 (3), 2008–2019.
Dikin, D.A., Stankovich, S., Zimney, E.J., Piner, R.D., Dommett, G.H., Evmenenko, G., Ruoff, R.S., 2007. Nature 448 (7152), 457–460.
Dreyer, D.R., Park, S., Bielawski, C.W., Ruoff, R.S., 2010. Chem. Soc. Rev. 39 (1), 228–240.
Dreyer, D.R., Todd, A.D., Bielawski, C.W., 2014. Chem. Soc. Rev. 43 (15), 5288–5301.
Forati, T., Atai, M., Rashidi, a.M., Imani, M., Behnamghader, 2014. Polym. Adv. Technol. 25, 322.
Ganesh, B.M., Isloor, A.M., Ismail, A.F., 2013. Desalination 313, 199.
Garg, Bhaskar, Bisht, Tanuja, Ling, Yong-Chien, 2014. Molecules 19 (9), 14582–14614.
Gómez-Navarro, C., Weitz, R.T., Bittner, A.M., Scolari, M., Mews, A., Burghard, M., Kern, K., 2007. Nano Lett. 7 (11), 3499–3503.
Gudarzi, M.M., Sharif, F., 2012. Express Polym. Lett. 6 (12).
He, H., Klinowski, J., Forster, M., Lerf, A., 1998. Chem. Phys. Lett. 287 (1), 53–56.
Heo, Y., Im, H., Kim, J., 2013. J. Membr. Sci. 425, 11–22.
Hu, H., Wang, X., Wang, J., Wan, L., Liu, F., Zheng, H., Xu, C., 2010. Chem. Phys. Lett. 484 (4), 247–253.
Huang, H.D., Ren, P.G., Xu, J.Z., Xu, L., Zhong, G.J., Hsiao, B.S., Li, Z.M., 2014. J. Membr. Sci. 464, 110–118.
Ionita, M., Pandele, A.M., Crica, L., Pilan, L., 2014. Compos. Part B Eng. 59, 133.
Jeon, Gil Woo, An, Ji-Eun, Jeong, Young Gyu, 2012. Compos. Part B: Eng. 43 (8), 3412–3418.
Jiang, Z., Zhao, X., Fu, Y., Manthiram, A., 2012. J. Mater. Chem. 22, 24862.
Jiang, Z., Zhao, X., Manthiram, A., 2013. Int. J. Hydrogen Energy 38, 5875.
Jin, T.X., Liu, C., Zhou, M., Chai, S.G., Chen, F., Fu, Q., 2015. Compos. Part A: Appl. Sci. Manuf. 68, 193–201.
Justin, R., Chen, B., 2014. Carbohydr. Polym. 103, 70.
Kabiri, Roya, Namazi, Hassan, 2014. Cellulose 21 (5), 3527–3539.
Kapantaidakis, G.C., Koops, G.H., 2002. J. Membr. Sci. 204, 153.
Kapantaidakis, G.C., Kaldis, S.P., Sakellaropoulos, G.P., Chira, E., Loppinet, B., Floudas, G., 1999. J. Polym. Sci. Pol. Phys. 37, 2788–2798.
Kim, D.H., Yun, Y.S., Jin, H.J., 2012. Curr. Appl. Phys. 12 (3), 637–642.
Lee, J., Chae, H.-R., Won, Y.J., Lee, K., Lee, C.-H., Lee, H.H., Kim, I.-C., Lee, J., 2013. J. Membr. Sci. 448, 223.
Lee, D.C., Yang, H.N., Park, S.H., Kim, W.J., 2014. J. Membr. Sci. 452, 20.
Lei, Z., Lu, L., Zhao, X.S., 2012. Energy Environ. Sci. 5 (4), 6391–6399.
Lerf, A., He, H., Forster, M., Klinowski, J., 1998. J. Phys. Chem. B 102 (23), 4477–4482.
Liu, Z., Wang, Y., Zhang, X., Xu, Y., Chen, Y., Tian, J., 2009. Appl. Phys. Lett. 94 (2), 021902.
Liu, M., Duan, Y., Wang, Y., Zhao, Y., 2014. Mater. Des. 53, 466–474.
Ma, J., Zhang, J., Xiong, Z., Yong, Y., Zhao, X.S., 2011. J. Mater. Chem. 21 (10), 3350–3352.
Marcano, D.C., Kosynkin, D.V., Berlin, J.M., Sinitskii, A., Sun, Z., Slesarev, A., Tour, J.M., 2010. ACS Nano 4 (8), 4806–4814.
Paredes, J.I., Villar-Rodil, S., Martinez-Alonso, A., Tascon, J.M.D., 2008. Langmuir 24 (19), 10560–10564.
Park, S., An, J., Jung, I., Piner, R.D., An, S.J., Li, X., Ruoff, R.S., 2009. Nano Lett. 9 (4), 1593–1597.

Park, O.-K., Kim, S.-G., You, N.-H., Ku, B.-C., Hui, D., Lee, J.H., 2014. Compos. Part B: Eng. 56, 365.
Pei, S., Cheng, H.-M., 2012. Carbon N.Y. 50, 3210.
Satti, A., Larpent, P., Gun'ko, Y., 2010. Carbon 48 (12), 3376–3381.
Shao, L., Chang, X., Zhang, Y., Huang, Y., Yao, Y., Guo, Z., 2013. Appl. Surf. Sci. 280, 989.
Sun, X., Liu, Z., Welsher, K., Robinson, J.T., Goodwin, A., Zaric, S., Dai, H., 2008. Nano Res. 1 (3), 203–212.
Szabó, T., Berkesi, O., Forgó, P., Josepovits, K., Sanakis, Y., Petridis, D., Dékány, I., 2006. Chem. Mater. 18 (11), 2740–2749.
Tseng, C.-Y., Ye, Y.-S., Cheng, M.-Y., Kao, K.-Y., Shen, W.-C., Rick, J., Chen, J.-C., Hwang, B., 2011. J. Adv. Energy Mater. 1, 1220.
Venugopal, G., Krishnamoorthy, K., Mohan, R., Kim, S.J., 2012. Mater. Chem. Phys. 132 (1), 29–33.
Voicu, S.I., Pandele, M.A., Vasile, E., Rughinis, R., Crica, L., Ionita, M., 2013. Dig. J. Nanomater. Bios. 8 (4), 1389.
Wang, H., Hao, Q., Yang, X., Lu, L., Wang, X., 2010. ACS Appl. Mater. Interfaces 2 (3), 821–828.
Wang, Y., Li, Z., Hu, D., Lin, C.T., Li, J., Lin, Y., 2010. J. Am. Chem. Soc. 132 (27), 9274–9276.
Wang, J.Y., Yang, S.Y., Huang, Y.L., Tien, H.W., Chin, W.K., Ma, C.C.M., 2011. J. Mater. Chem. 21 (35), 13569–13575.
Wang, N., Ji, S., Li, J., Zhang, R., Zhang, G., 2014. J. Membr. Sci. 455, 113.
Xu, Y., Bai, H., Lu, G., Li, C., Shi, G., 2008. J. Am. Chem. Soc. 130 (18), 5856–5857.
Xu, Z., Zhang, J., Shan, M., Li, Y., Li, B., Niu, J., Zhou, B., Qian, X., 2014. J. Membr. Sci. 458, 1.
Xu, Q., Xu, H., Chen, J., Lv, Y., Dong, C., Sreenivasan, T.S., 2015. Inorg. Chem. Front. 2, 417.
Yang, Y., Wang, P., Zheng, Q., 2006. J. Polym. Sci. Part B Polym. Phys. 44, 879.
Yuan, T., Pu, L., Huang, Q., Zhang, H., Li, X., Yang, H., 2014. Electrochim. Acta 117, 393.
Zhang, J., Cao, Y., Feng, J., Wu, P., 2012. J. Phys. Chem. C 116 (14), 8063–8068.
Zhang, Y., Mark, J.E., Zhu, Y., Ruoff, R.S., Schaefer, D.W., 2014. Polymer 55 (21), 5389–5395.
Zhao, H., Wu, L., Zhou, Z., Zhang, L., Chen, H., 2013. Phys. Chem. Chem. Phys. 15 (23), 9084–9092.
Zhao, C., Xu, X., Chen, J., Yang, F., 2013. J. Environ. Chem. Eng. 1, 349.
Zhao, C., Xu, X., Chen, J., Wang, G., Yang, F., 2014. Desalination 340, 59.
Zhu, Y., Murali, S., Cai, W., Li, X., Suk, J.W., Potts, J.R., Ruoff, R.S., 2010. Adv. Mater. 22 (35), 3906–3924.
Zhu, J., Lee, C.-H., Joh, H.-I., Kim, H.C., Lee, S., 2012. Carbon Lett. 13, 230.
Zinadini, S., Zinatizadeh, A.A., Rahimi, M., Vatanpour, V., Zangeneh, H., 2014. J. Membr. Sci. 453, 292.